This article has been accepted for publication in a future issue of this journal, but has not been fully edited. Content may change prior to final publication. Citation information: DOI 10.1109/TII.2018.2877143, IEEE Transactions on Industrial Informatics

Distributed Multi-Energy Coordination of Multi-Microgrids with Biogas-Solar-Wind Renewables

Da Xu, Bin Zhou, *Senior Member, IEEE*, Ka Wing Chan, *Member, IEEE*, Canbing Li, *Senior Member, IEEE*, Qiuwei Wu, *Senior Member, IEEE*, Biyu Chen, Shiwei Xia, *Member, IEEE*

***Abstract*—This paper proposes a distributed multi-energy management framework for the coordinated operation of interconnected biogas-solar-wind microgrids. In this framework, each microgrid not only schedules its local hybrid biogas-solar-wind renewables for coupled multi-carrier energy supplies based on the concept of energy hub, but also exchanges energy with interconnected microgrids and via the transactive market. The multi-microgrid scheduling is a challenging optimization problem due to its severe constraints and strong couplings. A multi-microgrid multi-energy coupling matrix is thus formulated to model and exploit the inherent biogas-solar-wind energy couplings among electricity, gas and heat flows. Furthermore, a distributed stochastic optimal scheduling scheme with minimum information exchange overhead is proposed to dynamically optimize energy conversion and storage devices in the multi-microgrid system. The proposed method has been fully tested and benchmarked on different scaled multi-microgrid system over a 24-hour scheduling horizon. Comparative results demonstrated that the proposed approach can reduce the system operating cost and enhance the system energy-efficiency, and also confirm its scalability in solving large-scale multi-microgrid problems.**

***Index Terms*—Energy hub, multi-energy couplings, distributed optimization, multi-microgrids, renewable energy.**

NOMENCLATURE

Indices and sets

iter	Index for iteration number
k	Index for time slots
n	Index for microgrids
s	Index for scenarios
x	Set of optimization variables

Parameters

C_z	Thermal capacitance of digester inside
C_{W1}, C_{W2}	Thermal capacitances of 1st and 2nd layer walls
E_R	Rated capacity of BES
G_{PVT}, W_{WT}, E_{bio}	Solar, wind, and biomass energy inputs
K_{end}	End time slot in a scheduling horizon
L_e, L_h, L_g	Electricity, heat/thermal, and gas loads
m, b	Coefficients of biogas production rate
$MFlow_{e,max}$, $MFlow_{g,max}$	Maximum capacities of power lines and gas pipelines
N_s	Total number of scenarios
P_{WT}	Wind power output
P_{PVT}, H_{PVT}	Electricity and thermal energy outputs of PVT
$P_{ch,max}$, $P_{dis,max}$	Maximum charging and discharging power of BES
Q_{bio}	Heating value of biogas
R_{in}, R_{out}	Thermal resistances for internal and external convective heat transfer
R_{W1}, R_{W2}	Thermal resistances for conductive heat transfer of the 1st and 2nd layer walls
$SOC_{bio,min}$, $SOC_{bio,max}$	Minimum and maximum bounds of SOC of biogas tank
$SOC_{BES,min}$, $SOC_{BES,max}$	Minimum and maximum values of SOC of BES
$S_{B,max}$, $S_{F,max}$	Maximum thermal outputs of boiler and furnace
$S_{CHP,max}$, $H_{CHP,max}$	Maximum electricity and thermal outputs of CHP
$T_{Z,min}$, $T_{Z,max}$	Minimum and maximum bounds of digestion temperature
$V_{GS,min}$, $V_{GS,max}$,	Minimum and maximum outputs of biogas storage tank
V_R	Rated capacity of biogas storage
$\eta_{e,CHP}$, $\eta_{h,CHP}$	Electrical and thermal efficiencies of CHP
η_B	Conversion efficiency of boiler
η_F	Conversion efficiency of furnace
η_{ch}, η_{dis}	Charging and discharging efficiencies of BES
μ_{BES}	Amortized cost of BES charging/discharging over the lifetime
μ_e, μ_g	Unit costs of electricity and biogas exchange
ρ_s	Probability of the occurrence of scenario *s*
a_e, a_g	Initial positive step size for electricity and biogas

Variables

$BC_{k,n}$	Battery degradation cost at the *k*th time slot in microgrid *n*
$P_{BES,k,n}$	Net outputs of BES at the *k*th time slot in microgrid *n*, i.e. $P_{dis,k,n}$ minus $P_{ch,k,n}$
$P_{dis,k,n}$, $P_{ch,k,n}$	Discharging and charging power of BES at the *k*th time slot in microgrid *n*
$PC_{k,n}$	Electricity procurement cost at the *k*th time slot in microgrid *n*
$S_{B,k,n}$, $S_{CHP,k,n}$, $S_{F,k,n}$	Outputs of electric boiler, CHP unit, and biogas furnace at time slot *k* in microgrid *n*
$S_{ef,k,n}$, $S_{hf,k,n}$	Electricity and thermal energy for digester heating

This work was jointly supported by the National Natural Science Foundation of China (51877072, 51507056), Hunan Strategic Industries Scientific and Technological Project under Grant 2017GK4028, Jiangsu Basic Research Project (Natural Science Foundation BK20180284), and Beijing Natural Science Foundation (3174057).

D. Xu, B. Zhou, and C. Li are with the College of Electrical and Information Engineering, Hunan University, Changsha 410082, China, and also with the Hunan Key Laboratory of Intelligent Information Analysis Integrated Optimization for Energy Internet, Hunan University, Changsha 410082, China (e-mail: binzhou@hnu.edu.cn).

K. W. Chan is with the Department of Electrical Engineering, The Hong Kong Polytechnic University, Hong Kong.

Q. Wu is with the Center for Electric Power and Energy, Department of Electrical Engineering, Technical University of Denmark, Kgs. Lyngby, 2800 Denmark.

B. Chen is with the College of Electrical Engineering, Guangxi University, Nanning 530004, China.

S. Xia is with the School of Electrical and Electronic Engineering, North China Electric Power University, Beijing 102206, China.

This article has been accepted for publication in a future issue of this journal, but has not been fully edited. Content may change prior to final publication. Citation information: DOI 10.1109/TII.2018.2877143, IEEE Transactions on Industrial Informatics

	at time slot k in microgrid n
$S_{\text{eout},k,n}$, $S_{\text{gout},k,n}$	Electricity and biogas delivered to other microgrids at time slot k in microgrid n
$S_{\text{buy},k,n}$, $S_{\text{sell},k,n}$	Electricity purchased/sold from/to electricity market at time slot k in microgrid n
$SC_{k,n}$, $SC_{k,s,n}$	Operating cost at current time slot k and operating cost of scenario s at time slot k in microgrid n
$SOC_{\text{BES},k,n}$	SOC of BES at the kth time slot in microgrid n
$SOC_{\text{bio},k,n}$	SOC of biogas storage at the kth time slot in microgrid n
$TC_{k,n}$	Energy transferring cost at the kth time slot in microgrid n
$T_{\text{Z},k,n}$	Digestion temperature at the kth time slot in microgrid n
$T_{\text{W1},k,n}$, $T_{\text{W2},k,n}$	Temperatures of the 1st and 2nd layer walls at the kth time slot in microgrid n, respectively;
$T_{\text{out},k,n}$	Temperature of digester outside at the kth time slot in microgrid n
$V_{\text{GS},k,n}$	Net outputs of biogas tank, i.e. biogas discharging when $V_{\text{GS},k,n} > 0$ and charging when $V_{\text{GS},k,n} < 0$
$\alpha_{\text{e},k}$, $\alpha_{\text{g},k}$	Lagrangian multipliers at kth time slot
$\mu_{\text{buy},k}$, $\mu_{\text{sell},k}$	Electricity price and feed-in price at kth time slot
ν_{B}, ν_{CHP}, ν_{F},	Dispatch factors of input energy carriers to electric boiler, CHP, furnace
ν_e, ν_h, ν_g	Dispatch factors of input energy carriers to electricity, thermal, and biogas load
$\varphi_{k,n}$, $\delta_{k,n}$	Binary variables that register the BES charging and discharging at the kth time slot in microgrid n
θ_{e}, θ_{g}	Step sizes for electricity and biogas energy

Functions

f_{WT}	Power conversion function of WT
$f_{\text{e,PVT}}$, $f_{\text{h,PVT}}$	Electrical and thermal functions of PVT
f_{D}	Biogas production rate

Vectors and Matrix

C	Coupling matrix
E	Input vector of energy hub
L	Output vector of energy hub

I. Introduction

A. Background and Motivation

Traditional microgrids are not interconnected and operate independently. Multiple microgrids can be interconnected to form a multi-microgrid system to further improve their reliability [1],[2]. Multi-microgrid system is clusters of distributed renewable energy sources (RESs), local loads, and energy storage systems in a distribution system where a distribution system operator (DSO) coordinates the energy scheduling of multiple microgrids [3]. Individually, the unpredictable effects caused by the RESs may be small in a microgrid as they may only contribute to a small portion of the overall energy generation. As the popularity of the microgrids is continuously growing, the uncertainty and unpredictability of solar and wind energy would become a concern on the integration and utilization of a high-penetration of renewables, and introduce operational challenges of multi-microgrid system.

Several recent representative literatures have studied the operation optimization of multi-microgrid system from various aspects, including optimal power dispatch [2]-[4], optimal voltage and frequency management [5], energy trading mechanism design [6]-[8], optimal power flow [9],[10], etc. With the increasing utilization of gas-fired and other distributed generation, especially co- and trigeneration, the electric microgrid gradually transforms towards a multi-energy microgrid. At the distribution system level, a multi-energy microgrid is comprised of distributed generation units such as wind turbines (WTs), photovoltaics (PVs), combined heat and power (CHP) or combined cooling, heat and power plants to simultaneously provide electricity and thermal energy supplies [11]. Biogas is a potential RES and is also becoming more and more appealing due to the growing demand of affordable and diversified energy services such as electricity, heating, and lighting [12],[13]. In [14], the optimal scheduling of hybrid RESs was investigated, in which the biogas-solar-wind complementarities are formed as a multi-energy microgrid for coupled multi-carrier energy supplies including electricity, heat, and gas. As an alternative to electricity, the renewable biogas can be used for electrical and thermal energy production in a CHP unit to satisfy local multi-energy loads, or be delivered to satisfy load demand in surrounding areas through gas pipeline [12]. This paper is devoted to further extend the microgrid in [14] to a biogas-solar-wind multi-microgrid system and form as an interconnected energy hub [15]-[17] to accommodate the variability of RESs and process multi-energy carriers.

The multi-microgrid scheduling involves not only the multi-energy scheduling of individual microgrids but also the multi-energy exchange among interconnected microgrids. In such cases, the coordinated operation of numerous microgrids would require a high bandwidth communication network for the acquisition of global information of the system characteristics. This could lead to a considerable amount of data traffic throughout the large-scale computing optimization scheme. Also, tracking these up-to-data information may be impractical since microgrids may not willing to share information with each other [6]. Therefore, the multi-microgrid scheduling is a challenging optimization problem which cannot be easily solved using conventional methods due to uncertainties of RESs, multi-energy couplings, high-dimensional variables, multi-energy demands, and limited communication bandwidth.

B. Literature Review

So far, extensive studies have been reported on coordinated operation of multi-microgrid system, enabling the active energy exchange via the power market and with interconnected microgrids. A distributed convex optimization framework was presented in [2],[6] for economic dispatch of islanded microgrids, and power exchange among microgrids to ensure the supply-demand balance all the time. Online energy management was proposed in [3], [18],[19] based on distributed algorithms to optimize their internal power devices and external energy trading with the electricity market and other microgrids. In [7],[20],[21], the game theory is used to introduce an incentive mechanism to encourage transactive energy trading and fair benefit sharing. However, so far those previous works focused only on systems with a single energy carrier. Regard-

This article has been accepted for publication in a future issue of this journal, but has not been fully edited. Content may change prior to final publication. Citation information: DOI 10.1109/TII.2018.2877143, IEEE Transactions on Industrial Informatics

ing to multi-energy microgrids, CHP-based microgrids at distribution network level was investigated in [8],[22], and a robust energy management system was designed to consider uncertainties associated with RES power outputs, time-varying load and energy prices. However, existing works have made the effort to enhance the system availability through electricity exchange among microgrids, and the role of gas exchange as well as the multi-energy couplings towards enhancing system operational availability were ignored. The multi-energy coordination and interactive multi-energy exchange of multiple microgrids are still not yet involved.

There are two types of multi-microgrid scheduling approaches proposed in the literatures. The first one is the centralized approach. The studies in [4],[20],[21] assumed a single centralized operator to coordinate supply and demand of all the microgrids, which may lead to privacy violations as well as computation and communication bottlenecks. The second one is the distributed approach in which distributed algorithms such as alternating directions method of multipliers algorithm [2],[3], Lagrangian relaxation [6], model predictive control [18],[19], consensus-algorithms [5],[23] have been proposed to solve this multi-microgrid scheduling problem. Nevertheless, existing distributed approaches have only been verified for their feasibility and effectiveness in operational optimization of systems employing only one form of energy, and few works have attempted to involve multiple energy carriers, such as electricity, heat and gas.

C. Contribution and Paper Organization

In this paper, the biogas-solar-wind energy couplings are explored and made use of to form a new coupled multi-carrier energy supply framework for interconnected microgrids. In this framework, each microgrid has independent optimization over its energy conversion and storage devices, and coordinates its operation with other microgrids for attaining the potential social benefits of multi-energy interconnection in the multi-microgrid system. The Lagrangian dual approach is then adopted to decentralize the multi-microgrid scheduling problem for solution efficiency and convergence performance. The contributions of this paper are summarized as follows:

1) An interconnected energy hub framework is proposed for the coordinated operation of multiple biogas-solar-wind microgrids. While previous works only focused on the electricity interconnection among microgrids, this study involves multi-energy interconnection and their potential benefits to the system operational efficiency are also analyzed.

2) A multi-microgrid multi-energy coupling matrix is formulated to model and exploit the inherent biogas-solar-wind energy couplings among microgrids. The couplings among electricity, gas and heat flows is subsequently decomposed into the internal multi-energy coordination within individual microgrids and external multi-energy exchange among interconnected microgrids for the improvement on the scheduling optimality and scalability.

3) A distributed stochastic optimal scheduling scheme with limited information exchange overhead is developed for the problem decomposition and iteratively converging to the optimal solution. Compared to the centralized scheme, the communication burden is lighter and information privacy is better protected since only the information in terms of multi-energy exchange is shared among microgrids.

The rest of the paper is organized as follows: Section II formulates the problem of multi-microgrid scheduling. Section III describes the proposed distributed stochastic optimal scheduling scheme. Section IV investigates and evaluates the performance of the proposed methodology through simulation studies. Section V presents the conclusions.

II. Problem Formulation

Due to the time-varying and location-dependent nature of RESs, one microgrid may have excess local renewable generation while another is short of energy supply. Also, users' energy consumption within different microgrids could be significantly different due to various types of consumers. The diversified renewable outputs and demand provide abundant opportunities for microgrids to exchange energy with each other to reduce system operating cost and enhance operational performance.

This paper aims to jointly optimize all the interconnected biogas-solar-wind microgrids to minimize their total operating cost while considering system operational uncertainties. The biogas-solar-wind renewables in an individual microgrid are intensively coupled based on the digesting thermodynamic effects [14]. With the digestion temperature effects on biogas production, the available electricity and thermal energy from renewable generations could be utilized for digester heating, thereby facilitating the anaerobic digestion process for biogas yield enhancement. The produced biogas can be stored in a compressed storage tank for later use in case of insufficient wind and solar energy. Electricity and biogas exchange among microgrids are also coupled with each other due to their mutual generation and transformation. Moreover, the coordinated operation of microgrids would require the DSO to be aware of all the operating technical specifications of each microgrid, which make the multi-microgrid system less scalable.

In order to take the full advantage of biogas-solar-wind renewables, the main objectives of this paper are to 1) model and exploit the multi-energy conversion and coupling relationship among different energy carriers, and 2) solve the multi-microgrid scheduling problem in a distributed way that can be solved with limited information exchange overhead.

A. Distributed Multi-Energy Management Framework

Fig. 1 illustrates a multi-microgrid system with interconnected biogas-solar-wind microgrids based on the concept of energy hub. The proposed distributed multi-energy management framework is supplied by biogas-solar-wind renewables that can be converted via WT, photovoltaic thermal (PVT) system and anaerobic digester into different energy carriers including electricity, heat and biogas. The PVT system consists of a thermal collector and PVs, and can generate both low-temperature heat and electricity simultaneously from solar energy [24]. In each microgrid, several energy conversion and storage devices are utilized to convert and/or condition these energy carriers into desirable qualities and quantities to meet the multi-energy demands. These microgrids are connected to the main power grid, and are also interconnected with each other through power lines and gas pipelines. The produced electricity and biogas are versatile and flexible energy carriers, which can either directly supply the local multi-energy

This article has been accepted for publication in a future issue of this journal, but has not been fully edited. Content may change prior to final publication. Citation information: DOI 10.1109/TII.2018.2877143, IEEE Transactions on Industrial Informatics

$$\underbrace{\begin{bmatrix} L_e \\ L_h \\ L_g \end{bmatrix}}_{\mathbf{L}_n} = \underbrace{\begin{bmatrix} f_{\mathrm{WT}}\nu_e & f_{e,\mathrm{PVT}}\nu_e & f_{\mathrm{D}}Q_{\mathrm{bio}}\nu_{\mathrm{CHP}}\eta_{e,\mathrm{CHP}}\nu_e & \nu_e & Q_{\mathrm{bio}}\nu_{\mathrm{CHP}}\eta_{e,\mathrm{CHP}}\nu_e \\ f_{\mathrm{WT}}\nu_{\mathrm{B}}\eta_{\mathrm{B}}\nu_h & (f_{e,\mathrm{PVT}}\nu_{\mathrm{B}}\eta_{\mathrm{B}}+f_{h,\mathrm{PVT}})\nu_h & f_{\mathrm{D}}Q_{\mathrm{bio}}(\nu_{\mathrm{CHP}}\eta_{e,\mathrm{CHP}}\nu_{\mathrm{B}}\eta_{\mathrm{B}}+\nu_{\mathrm{CHP}}\eta_{h,\mathrm{CHP}}+\nu_{\mathrm{F}}\eta_{\mathrm{F}})\nu_h & \nu_{\mathrm{B}}\eta_{\mathrm{B}}\nu_h & Q_{\mathrm{bio}}(\nu_{\mathrm{CHP}}\eta_{e,\mathrm{CHP}}\nu_{\mathrm{B}}\eta_{\mathrm{B}}+\nu_{\mathrm{CHP}}\eta_{h,\mathrm{CHP}}+\nu_{\mathrm{F}}\eta_{\mathrm{F}})\nu_h \\ 0 & 0 & f_{\mathrm{D}}\nu_{\mathrm{g}} & 0 & \nu_{\mathrm{g}} \end{bmatrix}}_{\mathbf{C}_{nn}} \underbrace{\begin{bmatrix} W_{\mathrm{WT}} \\ G_{\mathrm{PVT}} \\ E_{\mathrm{bio}} \\ P_{\mathrm{BES}} \\ V_{\mathrm{GS}} \end{bmatrix}}_{\mathbf{E}_n} \tag{1}$$

$$\underbrace{\begin{bmatrix} L_e \\ L_h \\ L_g \end{bmatrix}}_{\mathbf{L}_n} = \underbrace{\begin{bmatrix} 1 & 1 & 0 & 0 & 1 & 0 & -1/\eta_{\mathrm{B}} & 1 & 0 & -1 & 0 & -1 & 0 & 1 & -1 \\ 0 & 0 & 1 & 0 & 0 & 0 & 1 & \eta_{h,\mathrm{CHP}}/\eta_{e,\mathrm{CHP}} & 1 & 0 & -1 & 0 & 0 & 0 & 0 \\ 0 & 0 & 0 & f_{\mathrm{D}} & 0 & 1 & 0 & -1/Q_{\mathrm{bio}}\eta_{e,\mathrm{CHP}} & -1/Q_{\mathrm{bio}}\eta_{\mathrm{F}} & 0 & 0 & 0 & -1 & 0 & 0 \end{bmatrix}}_{\mathbf{C}'_{nn}} \underbrace{\begin{bmatrix} P_{\mathrm{WT}} \\ P_{\mathrm{PVT}} \\ H_{\mathrm{PVT}} \\ E_{\mathrm{bio}} \\ P_{\mathrm{BES}} \\ V_{\mathrm{GS}} \\ S_{\mathrm{B}} \\ S_{\mathrm{CHP}} \\ S_{\mathrm{F}} \\ S_{\mathrm{ef}} \\ S_{\mathrm{hf}} \\ S_{\mathrm{eout}} \\ S_{\mathrm{gout}} \\ S_{\mathrm{buy}} \\ S_{\mathrm{sell}} \end{bmatrix}}_{\mathbf{E}'_n} \tag{3}$$

demands of individual microgrid, or be delivered to supply other microgrids. Battery energy storage (BES) and biogas tank could provide large storage capacities for available electricity and biogas.

The DSO is a profit-neutral organization responsible for providing the microgrids with access to the market, and uses a two-way communication network to exchange necessary information with microgrids. It is assumed that the power buying/selling prices for all the microgrids are the same, and the electricity price would not be affected by the microgrids since their generation/demand is relatively small compared to the other electricity market participants. All microgrids belong to the same entity or different entities with common interests, and coordinate with each other to determine the amount of electricity purchased/sold from/to the electricity market.

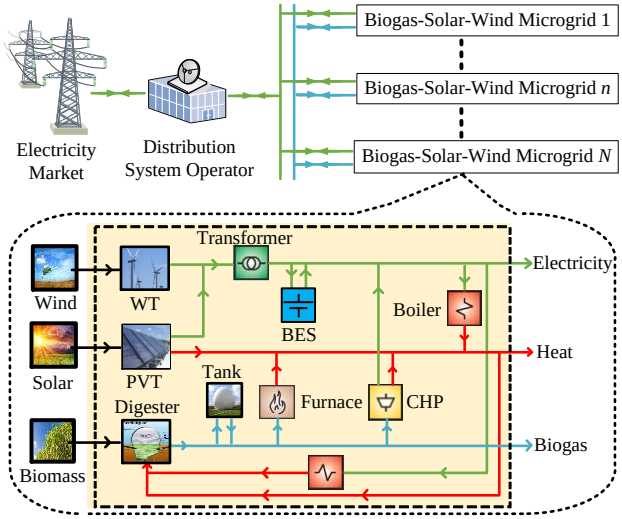

Fig. 1 Distributed biogas-solar-wind multi-energy management framework

B. Multi-Microgrid Multi-Energy Coupling Matrix

In order to analyze the inherent controllability and couplings, a coupling matrix is formulated to model the conversion and storage of different energy carriers within each microgrid, as shown in (1). The elements of coupling matrix are coupling factors, which represent the energy efficiencies and interior topology. The multi-energy coupling matrix of multi-microgrid system can thus be formulated, as follows,

$$\underbrace{\begin{bmatrix} L_1 \\ L_2 \\ \vdots \\ L_n \end{bmatrix}}_{\mathbf{L}} = \underbrace{\begin{pmatrix} C_{11} & C_{12} & \cdots & C_{1n} \\ C_{21} & C_{22} & \cdots & C_{2n} \\ \vdots & \vdots & \ddots & \vdots \\ C_{n1} & C_{n2} & \cdots & C_{nn} \end{pmatrix}}_{\mathbf{C}} \underbrace{\begin{bmatrix} E_1 \\ E_2 \\ \vdots \\ E_n \end{bmatrix}}_{\mathbf{E}} \tag{2}$$

In (2), the diagonal elements $\mathbf{C}_{nn}$ are obtained from (1) and represent internal multi-energy coordination within individual microgrids; the off-diagonal elements represent multi-energy exchange among interconnected microgrids and equal to $ag\{\nu_{ex},0,\nu_{gx}\}\mathbf{C}_{nn}$; ν_{ex} and ν_{gx} are dispatch factors of electricity and biogas from other microgrids to microgrid n. Also, each off-diagonal element is the negative of the corresponding element on the other side of the diagonal, e.g., $\mathbf{C}_{ij}$=-$\mathbf{C}_{ji}$.

The multi-microgrid multi-energy coupling model (1) and (2) are highly nonlinear and complex because of the introduction of dispatch factors. Thus, a state variable-based method in [16] is adopted to linearize the coupling matrix. Here, the outputs of energy conversion devices and the direct connections in Fig. 1 are designated as state variables. For instance, the biogas consumption of furnace, which is calculated by dispatch factor ν_{F} in (1), would be represented as $S_{\mathrm{F}}/\eta_{\mathrm{F}}$. As a result, a new state variable vector $\mathbf{E}'_n$ in (3) can be formed through combining all state variables with the input vector $\mathbf{E}_n$ in (1). Consequently, the coupling matrix $\mathbf{C}_{nn}$ can further be reformulated as an extended matrix $\mathbf{C}'_{nn}$ in (3) to indicate the inherent couplings among the input, output, and state variables. The multi-energy coupling matrix of multi-microgrid system can thus be formulated as a diagonal matrix, as follows,

This article has been accepted for publication in a future issue of this journal, but has not been fully edited. Content may change prior to final publication. Citation information: DOI 10.1109/TII.2018.2877143, IEEE Transactions on Industrial Informatics

$$\underbrace{\begin{bmatrix} L_1 \\ L_2 \\ \vdots \\ L_n \end{bmatrix}}_{\mathbf{L}} = \underbrace{\begin{pmatrix} C'_{11} & 0 & \cdots & 0 \\ 0 & C'_{22} & \cdots & 0 \\ \vdots & \vdots & \ddots & \vdots \\ 0 & 0 & \cdots & C'_{nn} \end{pmatrix}}_{\mathbf{C'}} \underbrace{\begin{bmatrix} E'_1 \\ E'_2 \\ \vdots \\ E'_n \end{bmatrix}}_{\mathbf{E'}} \tag{4}$$

In (4), the multi-energy exchange, which is calculated by the off-diagonal elements of (2), is decomposed to the state variable vector **E'** of (4). The multi-microgrid multi-energy coupling model (3) and (4) are linear and sparse for efficient computational iterations, and also exhibit more flexible for the scalability with the interconnection of microgrids.

C. Multi-Energy Scheduling of each Microgrid

The objective of each microgrid is to minimize its system operating cost $SC_{k,n}$ in the scheduling process, including electricity procurement cost $PC_{k,n}$, battery degradation cost due to the wear and tear incurred in charging/discharging actions $BC_{k,n}$ [7], energy transferring cost due to the electricity and biogas exchange $TC_{k,n}$ [25], as follows,

$$SC_{k,n} = PC_{k,n} + BC_{k,n} + TC_{k,n} \tag{5}$$

$$PC_{k,n} = \mu_{\text{buy},k} S_{\text{buy},k,n} - \mu_{\text{sell},k} S_{\text{sell},k,n} \tag{6}$$

$$BC_{k,n} = \mu_{\text{BES}} (P_{\text{ch},k,n} + P_{\text{dis},k,n}) \Delta k \tag{7}$$

$$TC_{k,n} = \mu_{\text{e}} S^2_{\text{eout},k,n} + \mu_{\text{g}} S^2_{\text{gout},k,n} \tag{8}$$

where μ_{BES} is the amortized cost of charging/discharging over the lifetime which can be calculated by battery capital cost, battery lifespan in the number of cycles, energy storage capacity, and reference depth-of-discharge according to [26]. The objective function is subject to the following constraints:

$$SOC_{\text{BES},k,n} = SOC_{\text{BES},k-\Delta k,n} + \frac{\eta_{\text{ch}} P_{\text{ch},k-\Delta k,n} \Delta k}{E_{\text{R},n}} - \frac{P_{\text{dis},k-\Delta k,n} \Delta k}{\eta_{\text{dis}} E_{\text{R},n}} \tag{9}$$

$$SOC_{\text{BES,min}} \le SOC_{\text{BES},k,n} \le SOC_{\text{BES,max}} \tag{10}$$

$$P_{\text{ch},k,n} \le P_{\text{ch},n,\max} \cdot \delta_{k,n} \tag{11}$$

$$P_{\text{dis},k,n} \le P_{\text{dis},n,\max} \cdot \varphi_{k,n} \tag{12}$$

$$\delta_{k,n} + \varphi_{k,n} \le 1 \tag{13}$$

$$SOC_{\text{bio},k,n} = SOC_{\text{bio},k-\Delta k,n} - \frac{V_{\text{GS},k-\Delta k,n}}{V_{R,n}} \tag{14}$$

$$SOC_{\text{bio,min}} \le SOC_{\text{bio},k,n} \le SOC_{\text{bio,max}} \tag{15}$$

$$V_{\text{GS},n,\text{min}} \le V_{\text{GS},k,n} \le V_{\text{GS},n,\max} \tag{16}$$

$$SOC_{j,1,n} = SOC_{j,K_{\text{end}},n} \quad (j = \text{BES,bio}) \tag{17}$$

$$f_{\text{D},n} = mT_{\text{Z},k,n} + b \tag{18}$$

$$C_{\text{Z},n} \frac{dT_{\text{Z},k,n}}{dk} = \eta_{\text{B}} S_{\text{ef},k,n} + S_{\text{hf},k,n} + \frac{T_{\text{W1},k,n} - T_{\text{Z},k,n}}{R_{\text{in},n} + R_{\text{W1},n}/2} \tag{19}$$

$$C_{\text{W1},n} \frac{dT_{\text{W1},k,n}}{dk} = \frac{T_{\text{Z},k,n} - T_{\text{W1},k,n}}{R_{\text{in},n} + R_{\text{W1},n}/2} + \frac{T_{\text{W2},k,n} - T_{\text{W1},k,n}}{R_{\text{W2},n}/2 + R_{\text{W1},n}/2} \tag{20}$$

$$C_{\text{W2},n} \frac{dT_{\text{W2},k,n}}{dk} = \frac{T_{\text{out},k,n} - T_{\text{W2},k,n}}{R_{\text{out},n} + R_{\text{W2},n}/2} + \frac{T_{\text{W1},k,n} - T_{\text{W2},k,n}}{R_{\text{W1},n}/2 + R_{\text{W2},n}/2} \tag{21}$$

$$T_{\text{Z,min}} \le T_{\text{Z},k,n} \le T_{\text{Z,max}} \tag{22}$$

$$0 \le S_{\text{B},k,n} \le S_{\text{B},n,\text{max}} \tag{23}$$

$$0 \le S_{\text{F},k,n} \le S_{\text{F},n,\text{max}} \tag{24}$$

$$\begin{cases} 0 \le S_{\text{CHP},k,n} \le S_{\text{CHP},n,\text{max}} \\ 0 \le S_{\text{CHP},k,n} \eta_{h,\text{CHP}} / \eta_{e,\text{CHP}} \le H_{\text{CHP},n,\text{max}} \end{cases} \tag{25}$$

$$\left| S_{\text{gout},k,n} \right| \le MFlow_{\text{g},n,\text{max}} \tag{26}$$

$$\begin{cases} \left| S_{\text{eout},k,n} \right| + \left| S_{\text{buy},k,n} \right| \le MFlow_{\text{e},n,\text{max}}, S_{\text{buy},k,n} \ge 0 \\ \left| S_{\text{eout},k,n} \right| + \left| S_{\text{sell},k,n} \right| \le MFlow_{\text{e},n,\text{max}}, S_{\text{sell},k,n} \ge 0 \end{cases} \tag{27}$$

Equations (9)-(17) show the constraints for charging, discharging, and SOC of BES and biogas storage, respectively. Equation (18) shows the constraints for biogas production rate which is modeled through fitting the experimental data in [12],[13],[27] with the polynomial regression. Equations (19)-(22) show the thermal balance constraints for digester inside, outside, and two-layer walls. In order to reduce computational complexity, the thermodynamics-based model in (19)-(22) is linearized around a nearest equilibrium point using the linearization method in [28]. The linearized state-space realization digester model can then be discretized for numerical iterations. It has been proved in [28],[29] that this linearization does not result in significant truncation error due to small temperature range within the digester. Equations (23)-(25) show the constraints for outputs of electric boiler, furnace, and CHP. Equations (26)-(27) show the energy security constraints for electricity and biogas.

D. Energy Exchange among Microgrids

Heterogeneous microgrids in general have different supply and demand profiles. Through exchanging energy with each other, microgrids can make full use of the flexibility and synergies of multi-energy supplies, and bring mutual benefits. A graph $G(M, A_e, A_g)$ is introduced to model the network topology of the system. Therein, $M = (m_1, m_2, m_3, \ldots, m_n)$ is a set of elements called nodes, $A_e = \{A_{e,ij} = (m_i, m_j)\} \subset M \times M$ and $A_g = \{A_{g,ij} = (m_i, m_j)\} \subset M \times M$ are a set of pairs of distinct nodes called edges. Graph nodes M represent the microgrids. The edges A_e and A_g represent the power lines and gas pipelines among microgrids, respectively. If there exists an edge $A_{e,ij}$ or $A_{g,ij}$ from microgrid i to microgrid j, it equals to 1; otherwise, it equals to 0. The multi-energy exchange in (4) can be calculated by the off-diagonal elements in (2), as follows,

$$S_{\text{eout},k,n} = -e_n^T A_e P_n \tag{28}$$

$$S_{\text{gout},k,n} = -e_n^T A_g V_n \tag{29}$$

where e_n is the nth column of the $N \times N$ identity matrix; $P_n = [v_{ex,1}\mathbf{C}_{11}\mathbf{E}_1, v_{ex,2}\mathbf{C}_{22}\mathbf{E}_2, \ldots, v_{ex,n-1}\mathbf{C}_{n-1n-1}\mathbf{E}_{n-1}, 0]^T$ and $V_n = [v_{gx,1}\mathbf{C}_{11}\mathbf{E}_1, v_{gx,2}\mathbf{C}_{22}\mathbf{E}_2, \ldots, v_{gx,n-1}\mathbf{C}_{n-1n-1}\mathbf{E}_{n-1}, 0]^T$ are all the electricity and biogas delivered from microgrid n to other microgrids, respectively. The sum of the exchanged electricity and biogas of all the microgrids should be equal to 0, as follows,

$$\sum_{n=1}^{N} S_{\text{eout},k,n} = 0 \tag{30}$$

$$\sum_{n=1}^{N} S_{\text{gout},k,n} = 0 \tag{31}$$

III. Distributed Stochastic Optimal Scheduling Scheme

In this study, a scenario-based stochastic scheduling with

This article has been accepted for publication in a future issue of this journal, but has not been fully edited. Content may change prior to final publication. Citation information: DOI 10.1109/TII.2018.2877143, IEEE Transactions on Industrial Informatics

rolling procedure [30] is implemented. Each rolling step solves for the current time slot and looks the remaining time slots ahead while considering the uncertainties of renewable generations and ambient temperature in future horizons. The objective is to minimize the system operating cost of all microgrids in the current time slot k and the expected operating cost of all microgrids in look-ahead time slots. A multi-microgrid scheduling model can thus be formulated to jointly optimize internal multi-energy coordination within individual microgrids and external multi-energy exchange among interconnected microgrids, as follows,

$$\min \left\{ \sum_{n=1}^{N} SC_{k,n} + \rho_s \Big(\sum_{k=k+\Delta k}^{K_{\text{end}}} \sum_{n=1}^{N} \sum_{s=1}^{N_s} SC_{k,s,n} \Big) \right\} \tag{32}$$

subject to constraints (3),(4),(9)-(31)

The cost minimization problem (32) for multi-microgrid system is centralized, and needs the information about the technical parameters of conversion and storage devices, renewable generations, multi-energy demands, etc. In order to safeguard critical information of microgrids and make the multi-microgrid system more scalable, a distributed stochastic optimal scheduling scheme is proposed to decompose the problem (32) into N local and reduced-complexity microgrid subproblems, and iteratively converge to the optimal solutions with limited information exchange overhead.

The multi-microgrid scheduling problem (32) is subject to two types of constraints, including local constraints (3),(9)-(29) involving local variables of each microgrid and coupling constraints (4),(30)-(31) involving variables of multiple microgrids. First of all, a Lagrangian relaxation approach is adopted for augmenting the centralized objective in (32) with coupling constraints (30)-(31). The Lagrangian function of the problem can then be defined as,

$$\begin{aligned} L(x, \alpha_{\text{e}}, \alpha_{\text{g}}) &= \sum_{n=1}^{N} SC_{k,n} + \alpha_{\text{e},k} \sum_{n=1}^{N} S_{\text{eout},k,n} + \alpha_{\text{g},k} \sum_{n=1}^{N} S_{\text{gout},k,n} \\ &= \sum_{n=1}^{N} [SC_{k,n} + \alpha_{\text{e},k} S_{\text{eout},k,n} + \alpha_{\text{g},k} S_{\text{gout},k,n}] \end{aligned} \tag{33}$$

where the first term expresses the objective of each microgrid; the last two terms are responsible for the coordination among the microgrids and are the contribution of microgrid n to the Lagrangian function; $\alpha_{\text{e},k}$ and $\alpha_{\text{g},k}$ are the Lagrangian multipliers associated with coupling constraints (30)-(31) at kth time slot. Then, Lagrangian function (33) can be expressed as,

$$L(x, \alpha_{\text{e}}, \alpha_{\text{g}}) = \sum_{n=1}^{N} L_n^{(l)}(x, \alpha_{\text{e}}, \alpha_{\text{g}}) \tag{34}$$

The dual of the problem is therefore defined by,

$$\min_{x} C(x) = \max_{\alpha_{\text{e}}, \alpha_{\text{g}}} C(\alpha_{\text{e}}, \alpha_{\text{g}}) \tag{35}$$

where $C(\alpha_{\text{e}}, \alpha_{\text{g}}) = \sum_{n=1}^{N} C_n^{(l)}(\alpha_{\text{e}}, \alpha_{\text{g}})$ with the local minimization subproblem

$$C_n^{(l)}(\alpha_{\text{e}}, \alpha_{\text{g}}) = \min_{x} C_n(x, \alpha_{\text{e}}, \alpha_{\text{g}}) \tag{36}$$

$$C_n(x, \alpha_{\text{e}}, \alpha_{\text{g}}) = L_n^{(l)}(x, \alpha_{\text{e}}, \alpha_{\text{g}}) + \sum_{s=1}^{N_s} \rho_s \Big(\sum_{k=k+\Delta k}^{K_{\text{end}}} L_n^{(l)}(x, \alpha_{\text{e}}, \alpha_{\text{g}}) \Big) \tag{37}$$

Due to the convexity of problem, the strong duality or Slater condition holds if there exists a feasible solution [31], and the optimal solution of the dual problem (35) is equal to the optimal solution of the primal problem (32). The problem can thus be solved in an iterative procedure: at each iteration, microgrid n solves the scenario-based stochastic optimization microgrid subproblem with fixed $\alpha_{\text{e},k}$ and $\alpha_{\text{g},k}$ to minimize its local operating cost; each microgrid exchanges information with DSO about the amount of electricity and biogas that it is willing to exchange with other microgrids; Lagrangian multipliers $\alpha_{\text{e},k,iter}$ and $\alpha_{\text{g},k,iter}$ are then updated, as follows,

$$\begin{bmatrix} \alpha_{\text{e},k,iter+1} \\ \alpha_{\text{g},k,iter+1} \end{bmatrix} = \begin{bmatrix} \alpha_{\text{e},k,iter} \\ \alpha_{\text{g},k,iter} \end{bmatrix} + \begin{bmatrix} \theta_{\text{e}} & 0 \\ 0 & \theta_{\text{g}} \end{bmatrix} \begin{bmatrix} \sum_{n=1}^{N} S_{\text{eout},k,n,iter} \\ \sum_{n=1}^{N} S_{\text{gout},k,n,iter} \end{bmatrix} \tag{38}$$

The iterations would stop in a time slot k when the change of variables $\alpha_{\text{e},k,iter}$ and $\alpha_{\text{g},k,iter}$ in two consecutive iterations is smaller than the tolerance δ. Five classical step-size rules are reported in [31] with proof of their convergence. In this study, a non-summable diminishing step size is adopted with conditions of $\theta > 0$, $\lim_{iter \to \infty} \theta = 0$, and $\sum_{iter=1}^{\infty} = \infty$, i.e. $\theta_{\text{e}} = a_e / \sqrt{iter}$, $\theta_{\text{e}} = a_g / \sqrt{iter}$.

After the iteration is converged, each microgrid obtained the scheduling decisions from the current time slot k to the end of the scheduling horizon K_{end}. Since each microgrid scheduling subproblem is performed with uncertainties in the upcoming time slots, microgrids only apply the obtained decision for the current time slot k, and would repeat the optimization procedure until the end of scheduling horizon to update its scheduling decision. Fig 2 illustrates the flowchart for implementation process of the proposed distributed stochastic optimal scheduling scheme. This procedure demonstrates the interaction among microgrids and DSO during the real-time operation of multi-microgrids system. Since only the coupling variables S_{eout}, S_{gout} need to be exchanged among microgrids and DSO, data traffic issues could be avoided, resulting in a more scalable approach.

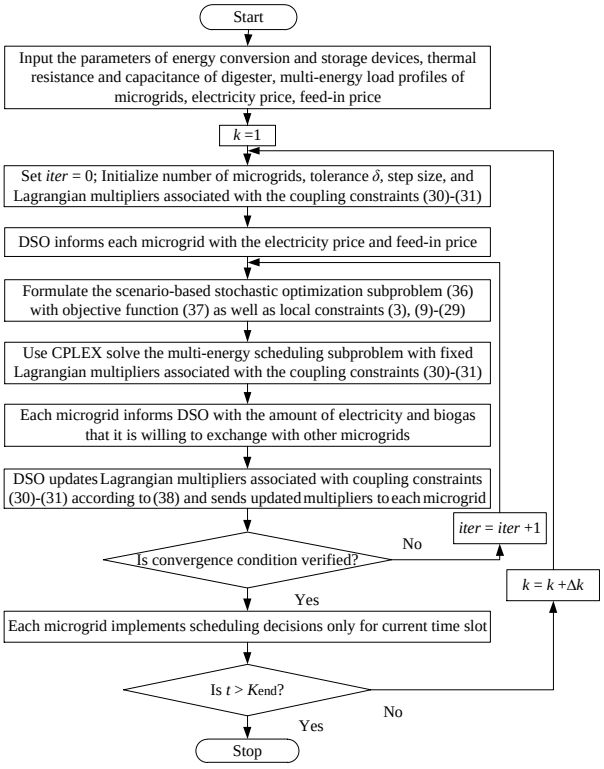

Fig. 2 Flowchart of distributed stochastic optimal scheduling scheme

This article has been accepted for publication in a future issue of this journal, but has not been fully edited. Content may change prior to final publication. Citation information: DOI 10.1109/TII.2018.2877143, IEEE Transactions on Industrial Informatics

IV. Case Studies

A. System Data

The proposed multi-energy coordination methodology is tested on a multi-microgrid system in Hunan, China, consisting of 3 biogas-solar-wind microgrids. The schematic diagram of the studied multi-microgrid system is illustrated in Fig.1. The electricity price of the main power grid is retrieved from [31]. Generally, feed-in price is lower than the electricity price so as to encourage local consumption of renewable energy, and thus reduce the impact on the main power grid. According to the feed-in tariff of distributed generation in most areas of China, the feed-in price is set as 0.01 $/kWh. In each microgrid, a 600m^3 in-ground tubular digester and a 600m^3 biogas storage tank are equipped. The rated capacities of PVT, WT, and BES of three microgrids are all 150kW, 400kW, and 400kWh, respectively. The daily electrical, thermal and gas load profiles of three microgrids are shown in Fig. 3-5, respectively. Noted that the gas load includes the biogas for domestic cooking and lighting. The base values of multi-energy load profiles are set as 350kW, 160kW, and 10m^3, respectively.

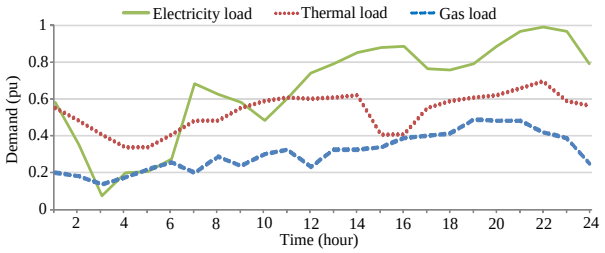

Fig. 3 Multi-energy load profiles of microgrid 1

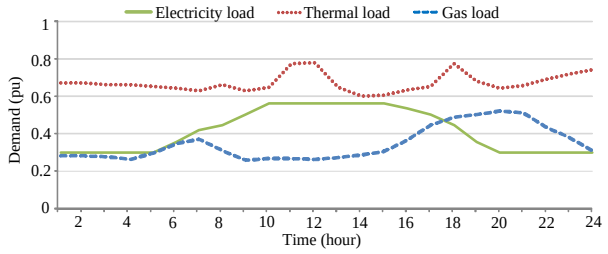

Fig. 4 Multi-energy load profiles of microgrid 2

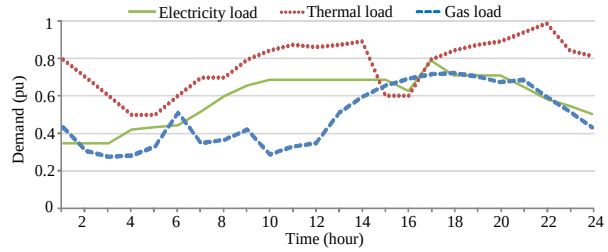

Fig. 5 Multi-energy load profiles of microgrid 3

The technical specifications of the three microgrids in this study are listed in Table I. The rolling horizon optimization of the multi-microgrid scheduling scheme is implemented over one day with 24 time slots. Here, the forecasted data of renewable generations as well as ambient temperature are obtained from the historical data using nonlinear regression methods, and their forecasting errors are selected to follow a normal distribution. A Monte Carlo approach in [32] is then performed to generate the original 100 scenarios with a corresponding possibility of 1/100 in each time slot. A scenario reduction method in [15] is further adopted to improve the computation efficiency, and only 10 scenarios are left for the microgrid scheduling.

TABLE I
Technical Specifications Of Microgrid Components In Hunan

Digester	$T_{Z,min}$= 20 ℃	$T_{Z,max}$= 40 ℃
	m = 2	a = 40
	Q_{bio}= 6.1 kWh/m^3	C_Z =749 kWh/ ℃
	C_{W1} =141.19 kWh/ ℃	C_{W2} =0.491 kWh/ ℃
	R_{in} =155.78×10^{-4} ℃/kW	R_{out} =50.71×10^{-4} ℃/kW
	R_{W1} =10.99×10^{-4} ℃/kW	R_{W2} =85.78×10^{-4} ℃/kW
Biogas storage	$V_{GS,min}$= -120 m^3	$V_{GS,max}$= 120 m^3
	$SOC_{bio,min}$= 0	$SOC_{bio,max}$= 1
Lead-acid BES	μ_{BES} = 0.01 $/kWh	η_{ch}= η_{dis}= 91.4%
	$SOC_{BES,min}$= 0.1	$SOC_{BES,max}$= 0.9
	$P_{ch,max}$=$P_{dis,max}$=80 kW	E_R= 400 kWh
CHP	$S_{CHP,1,max}$= 150 kW	
	$S_{CHP,2,max}$= 160 kW	$S_{CHP,3,max}$= 150 kW
	$\eta_{e,CHP}$= 0.4	$\eta_{h,CHP}$= 0.45
Boiler	$S_{B,1,max}$= 100 kW	$S_{B,2,max}$= 130 kW
	$S_{B,3,max}$= 140 kW	η_B= 0.75
Furnace	$S_{F,1,max}$= 150 kW	$S_{F,2,max}$= 180 kW
	$S_{F,3,max}$= 170 kW	η_F= 0.75
Unit cost	μ_e = 1e-5 $/(kW)^2	μ_g = 1e-4 $/(m^3)^2
Line capacity	$MFlow_{e,max}$= 400 kW	$MFlow_{g,max}$= 8 m^3

B. Comparative Results and Analysis

The comparative studies are implemented with three schemes: 1) Scheme 1 is the proposed distributed multi-energy coordination scheme in Sections II and III; 2) Scheme 2 is the multi-microgrid scheduling in the previous works [4],[6] in which biogas exchange among microgrids are not considered; 3) Scheme 3 performs the multi-microgrid scheduling without coordination in which electricity and biogas exchange among microgrids are not considered.

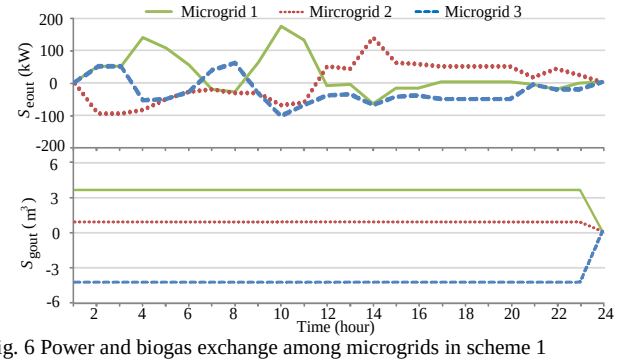

Fig. 6 Power and biogas exchange among microgrids in scheme 1

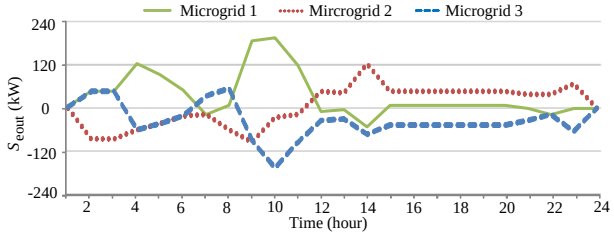

Fig. 7 Power exchange among microgrids in scheme 2

With the schemes 1-3, the curves of daily electricity and biogas exchange among microgrids as well as electricity procurement are illustrated in Fig. 6-8, respectively. Table II de-

This article has been accepted for publication in a future issue of this journal, but has not been fully edited. Content may change prior to final publication. Citation information: DOI 10.1109/TII.2018.2877143, IEEE Transactions on Industrial Informatics

scribes the comparative results of energy exchange and electricity buying/selling of three microgrids with the schemes 1-3. It can be found that all three microgrids not only purchased electricity from market but also interactively exchange electricity and biogas with each other across the 24-hour operation horizon. As the multi-energy loads are high and outputs of renewables are relatively low during hours 0-8, microgrids have to purchase more electricity from the market than other hours. Due to the low feed-in price and large storage capacities of BES as well as biogas storage, microgrids do not sell electricity to market. The multi-energy interconnection of microgrids indeed enable multi-microgrid system to cope with uncertainties by their own. The available renewable energy is delivered from microgrid 1 to other two microgrids during hours 1-12 and from microgrid 2 to other two microgrids during hours 13-24. Since the thermal load and gas load of microgrid 3 is larger than that of microgrid 1 and 2, the available biogas from microgrid 1 and 2 are supplied to microgrid 3 during the whole day. Though energy exchange among microgrids incur additional costs, microgrids in scheme 1 purchases less electricity from the main grid than scheme 2 and 3 and thus reduces their operating costs.

TABLE II
COMPARATIVE ANALYSIS OF ENERGY EXCHANGE AND ELECTRICITY SELLING/BUYING OF THREE MICROGRIDS OF SCHEME 1-3

Microgrid	Scheme 1			Scheme 2			Scheme 3		
	1	2	3	1	2	3	1	2	3
Electricity selling (kWh)	0	0	0	0	0	0	0	0	0
Electricity buying (kWh)	669.8	1843.4	905.7	628.3	1753.6	1227.0	125.6	1625.6	2191.4
Electricity exchange (kWh)	547.4	50.6	-598.0	844.7	82.5	-927.2	0	0	0
Biogas exchange (m^3)	75.1	20.3	-95.4	0	0	0	0	0	0
System operating cost	32.5	65.3	42.4	28.7	59.6	69.0	12.6	50.6	154.2

Fig. 9-13 illustrate the output curves of BES, biogas storage, CHP, boiler and furnace of three microgrids in schemes 1-3. It can be found that compared with schemes 2 and 3, the proposed methodology can achieve a better coordination of internal multi-energy scheduling and external energy exchange. For example, during the hours 15-20, the outputs of BES and CHP in scheme 1 increase to meet the soaring loads while the furnace stays unchanged. With the exchanged energy among microgrids, the BES and CHP in scheme 1 slightly decreases its output to follow the on-peak loads during the hours 21-24. However, in scheme 3, the furnace has to sharply increase its output while BES has run out of its power in advance. Also, microgrids have to purchase large amount of electricity from main grid which increases the system operating cost drastically. Besides, it can also be seen from Fig. 9 that at the beginning of the day, more power is stored into BES with energy exchange than that of without energy exchange. This is because microgrids can exchange available power with other microgrids, and thus charge more power in BES to meet their peak loads later. Furthermore, due to its high energy efficiency and cogeneration of electricity and heat, the CHP is prioritized as the energy supply unit in microgrids during hours 17-21.

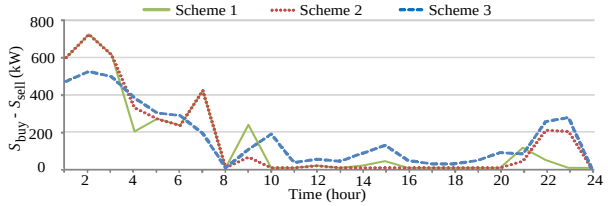

Fig. 8 Net power procurement in scheme 1-3

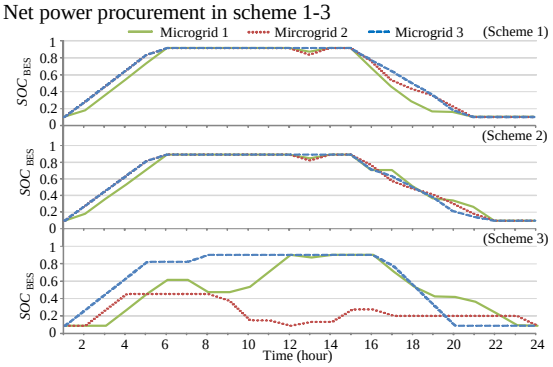

Fig. 9 SOC of BES of microgrids in schemes 1-3

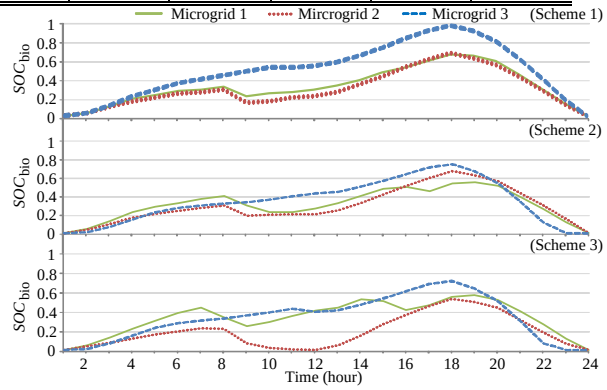

Fig. 10 SOC of biogas storage of microgrids in schemes 1-3

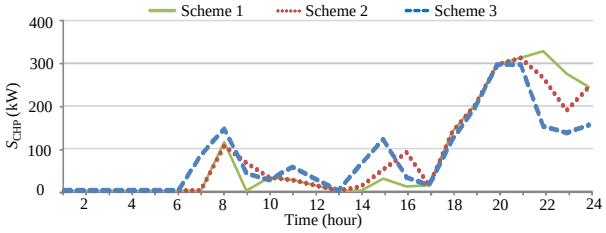

Fig. 11 Daily outputs of CHP in schemes 1-3

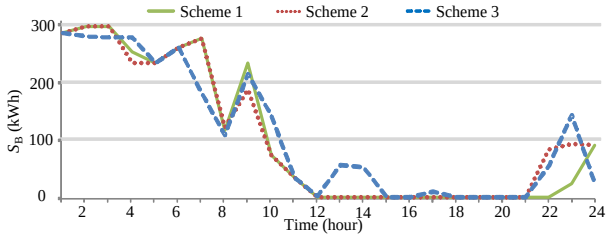

Fig. 12 Daily outputs of boiler in schemes 1-3

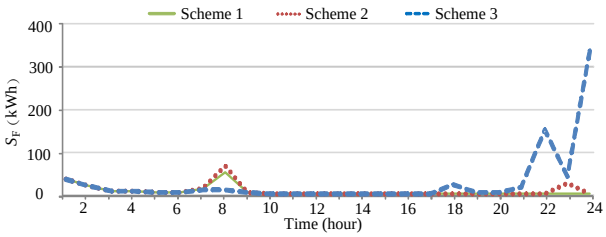

Fig. 13 Daily outputs of furnace in schemes 1-3

This article has been accepted for publication in a future issue of this journal, but has not been fully edited. Content may change prior to final publication. Citation information: DOI 10.1109/TII.2018.2877143, IEEE Transactions on Industrial Informatics

Table III lists the comparative results of schemes 1-3 on operating cost, biogas yield, battery degradation cost, total energy loss, and electricity procurement. Noted that the energy loss in this study includes the electrical energy losses and thermal energy losses of various converters and storages. It can be found that, compared with schemes 2 and 3, scheme 1 can supply different energy demands with higher energy efficiency and lower electricity procurement. Compared with the scheme 2, the energy loss can decline by 3.57 % with the proposed scheme, while the system operating cost can decrease by 10.83 %. With respect to the scheme 3, the energy loss and system operating cost are 10.94 % and 35.48 % with the scheme 1, respectively.

It is also observed that the proposed methodology can provide flexible multi-energy conversion and storage to improve the overall utilization of local renewable energy. Because of the power loss as well as wear and tear from charging/discharging actions of BES, microgrids in scheme 3 prefer to purchase more electricity from market, and leads to the less degradation cost in Table III. All in all, the comparative results can demonstrate the superior performance of the proposed scheme 1 on efficient energy management of multiple microgrids, especially on the improvements on operating cost and energy efficiency.

TABLE III
COMPARATIVE PERFORMANCE RESULTS OF SCHEMES 1-3

Scheme	1	2	3
System operating cost ($)	**140.26**	157.29	217.39
Biogas yield (m^3)	1119.90	1138.22	**1182.96**
Battery degradation cost ($)	20.25	20.25	**18.62**
Energy loss (kWh)	**2025.79**	2100.76	2274.72
Electricity procurement(kWh)	**3418.87**	3608.86	3942.58

C. Influence of Line Capacity

In order to analyze the effects of line capacity on the system performance, the proposed scheme is performed under different capacities of each microgrid varying from 0.3 per unit to 1 per unit with the base capacity 500kW. It can be noted from Fig. 6 that biogas can be easily compressed or delivered through pipelines, and their capacities are usually large enough to satisfy the demands of biogas exchange among microgrids. Fig. 14 illustrates the performance results of power procurement, electricity procurement cost, battery degradation cost and system operation cost considering different line capacities.

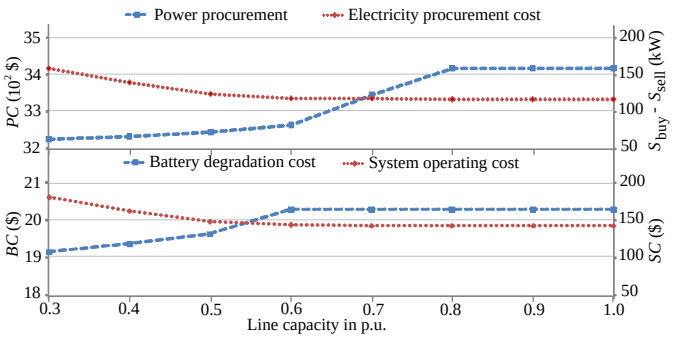

Fig. 14 system performance results versus different line rating

When the line capacity is below 0.3 per unit, energy inadequacy would occur, and load shedding is required to introduce to guarantee the supply-demand balance. With the increase of line capacity from 0.3 to 0.8 per unit, the electricity procurement cost *PC* gradually decreases though power procurement gradually increases. This is because larger line capacity enables microgrids could purchase more electricity under off-peak hours. In such cases, the battery degradation cost *BC* gradually increases while the system operation cost *SC* gradually decreases. When the line capacity is above 0.8 per unit, all the performance metrics remain unchanged. The results confirm that electricity and biogas exchange among microgrids can facilitate the utilization of high penetration of variable and intermittent RESs.

D. Discussion

A comparative study of the optimization results over 50 optimization runs for three schemes is given in Table IV. Five typical performance metrics, including the best solution, worst solution, average solution, standard deviation, and variance, are adopted to measure the solution performance. Due to the intermittent and volatile nature of renewable generations, the outputs of energy conversion and storage devices may slightly fluctuate, resulting in the fluctuations of the optimization results. The resulting statistics demonstrated that the proposed approach can provide satisfactory solutions, and further verify the stability of the proposed approach.

TABLE IV
RESULTING STATISTIC OF OPTIMIZATION RESULTS OF SCHEMES 1-3

Scheme	Best	Worst	Average	Variance	Std. Dev.
1	140.26	145.15	142.47	1.75	1.32
2	157.29	162.67	160.22	2.65	1.63
3	217.39	222.67	220.49	2.14	1.46

TABLE V
COMPARISONS OF AVERAGE CPU TIME FOR DIFFERENT APPROACHES

Number of microgrids	CPU time(s)	
	Proposed approach	Centralized approach
3	13	25
100	401	505
200	812	989
400	1602	2622
600	2399	5126
800	3195	9988
1000	4025	20955

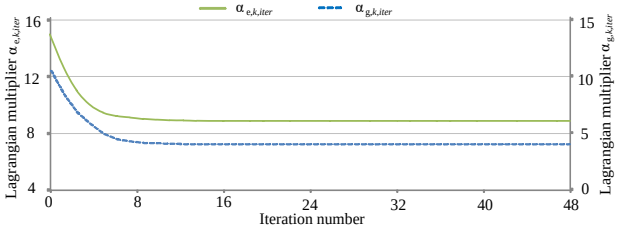

Fig. 15 Convergence of Lagrangian multipliers at hour 1

In order to demonstrate the superior performance of the proposed approach on multi-microgrid scheduling problems, a number of multi-microgrid systems with the number of microgrids varied from 3 to 1000 were scheduled using the pro-posed distributed approach and a centralized approach. Both approaches are implemented with YALMIP toolbox [33] running under MATLAB R2010a and solved using the MIQP

solver CPLEX on a personal computer with 4-GHz Intel Core i7 CPU and 8GB RAM. The CPLEX is a commercial software package, which can efficiently handle the numeric difficulties of linear programming automatically and solve many types of optimization problems. Fig. 15 shows the convergence of Lagrangian multipliers $\alpha_{e,k,iter}$ and $\alpha_{g,k,iter}$ at hour 1 of the three-microgrid system. The initial step size a_e and a_g are 0.001 and 0.2. It can be found that the multipliers converge to their optimum values within about 20 iterations. Due to the convexity of the problem, the two approaches converge to the same optimal solution, and the run time is thus adopted to measure and evaluate their solution efficiency. The comparative studies of two approaches on average CPU time are given in Tables V. While the run time of proposed approach increases linearly with the number of microgrids, the running time of centralized approach increases quadratically with the number of microgrids as a result of requiring a third party to collect all the necessary information. It can be concluded that the proposed approach can be used in scenarios with large number of microgrids.

V. Conclusion

In this paper, a distributed multi-energy management framework is proposed to solve the coordinated operation problem with heterogeneous microgrids. The multi-microgrid scheduling is decomposed into local and reduced-complexity microgrid subproblems, and a distributed stochastic optimal scheduling scheme with minimum information exchange overhead is developed to iteratively solve this problem. The effectiveness and validity of the proposed methodology have been extensively tested on multi-microgrid systems with the number of microgrids varied from 3 to 1000. The conclusions of this investigation are summarized as follows: 1) The proposed method can effectively handle the uncertainties of intermittent and volatile RESs with the multi-energy coordination and interactive exchange among microgrids; 2) The proposed method can significantly outperform other methods, and demonstrates its superiority on various performance metrics, especially on system operating cost reduction and energy-efficiency enhancement; 3) The proposed scheduling procedure only requires microgrids to share limited information and encourage them to independently optimize their own objectives with locally available information; 4) Compared with a centralized approach, the proposed distributed approach has a considerably lower computational time and avoid any privacy issue, and further validated its scalability in solving large-scale multi-microgrid problems. Further on-going research would focus on the participation of multi-microgrid system as a price-maker in the real-time electricity market.

References

[1] M. Shahidehpour, Z. Li, S. Bahramirad, Z. Li, and W. Tian, "Networked microgrids: exploring the possibilities of the IIT-Bronzeville grid," *IEEE Power Energy Mag*., vol. 15, no. 4, pp. 63–71, Jul./Aug. 2017.

[2] G. Chen and Q. Yang, "An ADMM-based distributed algorithm for economic dispatch in islanded microgrids," *IEEE Trans. Ind. Informat*., DOI: 10.1109/TII.2017.2785366, in press, 2017.

[3] W. Ma, J. Wang, V. Gupta, and C. Chen, "Distributed energy management for networked microgrids using online alternating direction method of multipliers with regret," *IEEE Trans. Smart Grid*, vol. 9, no. 2, pp. 847–856, Mar. 2018.

[4] S. Wang, H. Gangammanavar, and S. D. Ekşioğlu, *et al*., "Stochastic optimization for energy management in power systems with multiple microgrids," *IEEE Trans. Smart Grid*, DOI: 10.1109/TSG.2017.2759159, in press, 2017.

[5] Z. Li, C. Zang, and P. Zeng, *et al*., "Fully distributed hierarchical control of parallel grid-supporting inverters in islanded AC microgrids," *IEEE Trans. Ind. Informat*., vol. 14, no. 2, pp. 679-690, Feb. 2018.

[6] D. Gregoratti and J. Matamoros, "Distributed energy trading: the multiple-microgrid case," *IEEE Trans. Ind. Electron.*, vol. 62, no. 4, pp. 45–53, Apr. 2015.

[7] H. Wang and J. Huang, "Incentivizing energy trading for interconnected microgrids," *IEEE Trans. Smart Grid*, DOI: 10.1109/TSG.2016.2614988, in press, 2016.

[8] C. Li, Y. Xu, and X. Yu, *et al*., "Risk-averse energy trading in multi-energy microgrids: a two-stage stochastic game approach," *IEEE Trans. Ind. Informat*., vol. 13, no. 5, pp. 2620-2630, Oct. 2017.

[9] W. Zhang, Y. Xu, Z. Dong, and K. P. Wong, "Robust security constrained-optimal power flow using multiple microgrids for corrective control of power systems under uncertainty," *IEEE Trans. Ind. Informat*., vol. 13, no. 4, pp. 1704–1713, Aug. 2017.

[10] E. Dall'Anese, H. Zhu, and G. B. Giannakis, "Distributed optimal power flow for smart microgrids," *IEEE Trans. Smart Grid*, vol. 4, no. 3, pp. 1464–1475, Sep. 2013.

[11] C. Zhang, Y. Xu, and Z. Li, et al., "Robustly coordinated operation of a Multi-energy microgrid with flexible electric and thermal Loads," *IEEE Trans. Smart Grid*, DOI: 10.1109/TSG.2018.2810247, in press, 2018.

[12] C. Mao, Y. Feng, and X. Wang, *et al*., "Review on research achievements of biogas from anaerobic digestion," *Renew. Sustain. Energy Rev.*, vol. 45, pp. 540-555, May 2015.

[13] R. Feng, J. Li, and T. Dong, "Performance of a novel household solar heating thermostatic biogas system," *Appl. Thermal Eng*., vol. 96, pp. 519-526, Mar. 2016.

[14] B. Zhou, D. Xu, C. B. Li, C. Y. Chung, Y. J. Cao, K. W. Chan, and Q. W. Wu, "Optimal scheduling of biogas-solar-wind renewable portfolio for multi-carrier energy supplies," *IEEE Trans. Power Syst*., DOI: 10.1109/TPWRS.2018.2833496, in press, 2018.

[15] A. Dolatabadi, B. Mohammadi-ivatloo, M. Abapour, and S. Tohidi, "Optimal stochastic design of wind integrated energy hub," *IEEE Trans. Ind. Informat*., vol. 13, no. 5, pp. 2379-2388, Oct. 2017.

[16] C. Shao, X. Wang, and M. Shahidehpour, et al., "An MILP-based optimal power flow in multicarrier energy systems," *IEEE Trans. Sustain. Energy*, vol. 8, no. 1, pp. 239-248, Jan. 2017.

[17] M. Geidl and G. Andersson, "Optimal power flow of multiple energy carriers," *IEEE Trans. Power Syst.*, vol. 22, no. 1, pp. 145-155, Feb. 2007.

[18] F. Garcia-Torres, C. Bordons, and M. A. Ridao, "Optimal economic schedule for a network of microgrids with hybrid energy storage system using distributed model predictive control," *IEEE Trans. Ind.* Electron., DOI: 10.1109/TIE.2018.2826476, in press, 2018.

[19] K. Utkarsh, D. Srinivasan, and A. Trivedi, *et al*., "Distributed model-predictive real-time optimal operation of a network of smart microgrids," *IEEE Trans. Smart Grid*, DOI: 10.1109/TSG.2018.2810897, in press, 2018.

[20] Y. Z. Li, T. Y. Zhao, and P. Wang, *et al*. "Optimal Operation of Multi-Microgrids via Cooperative Energy and Reserve Scheduling," *IEEE Trans. Ind. Informat*., DOI: 10.1109/TII.2018.2792441, in press, 2018.

[21] M. M. Esfahani, A. Hariri, and O. A. Mohammed, "A multiagent-based game-theoretic and a multiagent-based game-theoretic and multi-microgrid systems," *IEEE Trans. Ind. Informat*., DOI: 10.1109/TII.2018.2808183, in press, 2018.

[22] A. Parisio, C. Wiezorek, and T. Kynt ̈aj ̈a, *et al*., "Cooperative MPC-based Energy Management for Networked Microgrids," *IEEE Trans. Smart Grid*, DOI: 10.1109/TSG.2017.2726941, in press, 2018.

[23] A. Pilloni, A. Pisano, and E. Usai, "Robust finite-time frequency and voltage restoration of inverter-based microgrids via sliding-mode cooperative control," *IEEE Trans. Ind.* Electron., vol. 65, pp. 1, Jan. 2018.

[24] S. Thakare, K. Priya, C. Ghosh, and S. Bandyopadhyay, "Optimization of photovoltaic-thermal based cogeneration system through water replenishment profile," *Solar Energy*, vol. 133, pp. 512-523, Aug. 2016.

[25] D. Alkano and J. Scherpen, "Distributed supply coordination for power-to-gas facilities embedded in energy grids," *IEEE Trans. Smart Grid*, DOI: 10.1109/TSG.2016.2574568, in press, 2016.

[26] W. Kempton and J. Tomi´c, "Vehicle-to-grid power fundamentals: Calculating capacity and net revenue," *J. Power Sources*, vol. 144, pp. 268-279, Apr. 2005.

[27] X. Pu, L. Deng, and Y. Yin, *et al*. "Economic benefit analysis on large and middle-scale biogas plants with different heating methods," *Transactions of the CSAE*, vol. 26, no. 7, pp. 281-284, July 2010. (in Chinese)
[28] W. J. Mai and C. Y. Chung, "Economic MPC of aggregating commercial buildings for providing flexible power reserve," *IEEE Trans. Power Syst.*, vol. 30, no. 5, pp. 2685-2694, Sep. 2015.
[29] M. Maasoumy, Controlling energy-efficient buildings in the context of smart grid: a cyber physical system approach Univ. California, Elect. Eng. Dept., Berkeley, 2013, Tech. Rep. UCB/EECS-2013-244.
[30] R. Palma-Behnke, C. Benavides, and F. Lanas, *et al*., "A Microgrid energy management system based on the rolling horizon strategy," *IEEE Trans. Smart Grid*, vol. 4, no. 2, pp. 996-1006, June 2013.
[31] S. Boyd and L. Vandenberghe, "Convex optimization," Cambridge University Press, 2004
[32] B. Zhou, D. Xu, and K. W. Chan, *et al.* "A two-stage framework for multiobjective energy management in distribution networks with a high penetration of wind energy," *Energy*, vol. 135, pp. 754-766, Jul. 2017.
[33] J. Löfberg, "YALMIP: A toolbox for modeling and optimization in MATLAB," in *Proc. CACSD Conf*., 2004, pp. 284-289.

Da Xu received the B.Sc. degree in automation from Wuhan University of Technology, Wuhan, China, in 2015. He is currently pursuing the Ph.D. degree at the College of Electrical and Information Engineering in Hunan University, Changsha, China. His major research interests include smart grid operation and optimization, renewable energy generation.

Bin Zhou (S'11-M'13-SM'17) received the B.Sc. degree in electrical engineering from Zhengzhou University, Zhengzhou, China, in 2006, the M.S. degree in electrical engineering from South China University of Technology, Guangzhou, China, in 2009, and the Ph.D. degree from The Hong Kong Polytechnic University, Hong Kong, in 2013. Afterwards, he worked as a Research Associate and subsequently a Postdoctoral Fellow in the Department of Electrical Engineering of The Hong Kong Polytechnic University. Now, he is an Associate Professor in the College of Electrical and Information Engineering, Hunan University, Changsha, China. His main fields of research include smart grid operation and planning, renewable energy generation, and energy efficiency.

Ka Wing Chan (M'98) received the B.Sc. (with First Class Honors) and Ph.D. degrees in electronic and electrical engineering from the University of Bath, Bath, U.K., in 1988 and 1992, respectively. He currently is an Associate Head and Associate Professor in the Department of Electrical Engineering of The Hong Kong Polytechnic University. His general research interests include smart grid and renewable energy, power system stability analysis and control, power system planning and optimization, real-time power system simulation.

Canbing Li (M'06-SM'13) received the B.Sc. degree and the Ph.D. degree both in electrical engineering from Tsinghua University, Beijing, China, in 2001 and 2006, respectively. He is currently a Professor with the College of Electrical and Information Engineering, Hunan University, Changsha, China. His research interests include smart grid, energy efficiency and energy policy.

Qiuwei Wu (M'08-SM'15) obtained the PhD degree in Power System Engineering from Nanyang Technological University, Singapore, in 2009. He was a senior R&D engineer with VESTAS Technology R&D Singapore Pte Ltd from Mar. 2008 to Oct. 2009. He has been working at Department of Electrical Engineering, Technical University of Denmark (DTU) since Nov. 2009 (PostDoc Nov. 2009-Oct. 2010, Assistant Professor Nov. 2010-Aug. 2013, Associate Professor since Sept. 2013). He was a visiting scholar at Department of Industrial Engineering & Operations Research (IEOR), University of California, Berkeley, from Feb. 2012 to May 2012 funded by Danish Agency for Science, Technology and Innovation (DASTI), Denmark. He was a visiting professor named by Y. Xue, an Academician of Chinese Academy of Engineering, at Shandong University, China, from Nov. 2015 to Oct. 2017. Currently, he is a visiting scholar at the Harvard China Project, School of Engineering and Applied Sciences, Harvard University. His research interests are operation and control of power systems with high penetration of renewables, including wind power modelling and control, actve distribution networks, and operation of integrated energy systems. He is an Editor of IEEE Transactions on Smart Grid and IEEE Power Engineering Letters.

Biyu Chen received the B.Sc. degree in electrical engineering from South China University of Technology, Guangzhou, China, in 1999, the M.S. degree in electrical engineering from Guangxi University, Nanning, China, in 2003, and the Ph.D. degree from South China University of Technology, Guangzhou, China, in 2006. Now, she is an Associate Professor in the College of Electrical Engineering, Guangxi University, Nanning, China. Her main fields of research include smart grid operation, control and reliability.

Shiwei Xia (M'12) received the B.Eng. and M.Eng. degrees in electrical engineering from Harbin Institute of Technology, Harbin, China, in 2007 and 2009 respectively, and the Ph.D. degree in power systems from The Hong Kong Polytechnic University, Hung Hom, Hong Kong, in 2015. Then, he worked as a Research Associate and subsequently as a Postdoctoral Fellow with the Department of Electrical Engineering, The Hong Kong Polytechnic University, in 2016-2018. Currently, he is a lecturer in the School of Electrical and Electronic Engineering, North China Electric Power University, Beijing. His research interests include distributed optimization and control of multiple sustainable energy sources in active distribution network.